Journal of Physiology - Paris 103 (2009) 306–314

Contents lists available at ScienceDirect

Journal of Physiology - Paris

journal homepage: www.elsevier.com/locate/jphysparis

Improving the SNR of EEG generated by deep sources with weighted multielectrode leads

Outi Väisänen *, Jaakko Malmivuo

Department of Biomedical Engineering, Tampere University of Technology, P.O. Box 692, FIN-33101 Tampere, Finland

ARTICLE INFO

Keywords:
Multielectrode EEG lead
Lead field theory
Sensitivity distribution
Deep EEG sources
Signal-to-noise ratio

ABSTRACT

We have developed a multielectrode lead technique to improve the signal-to-noise ratio (SNR) of scalp-recorded electroencephalography (EEG) signals generated deep in the brain. The basis of the method lies in optimization of the measurement sensitivity distribution of the multielectrode lead. We claim that two factors improve the SNR in a multielectrode lead: (1) the sensitivity distribution of a multielectrode lead is more specific in measuring signals generated deep in the brain and (2) spatial averaging of noise occurs when several electrodes are applied in the synthesis of a multielectrode lead. We showed theoretically that within a three-layer spherical head model the sensitivity distributions of multielectrode leads are more specific for deep sources than those of traditional bipolar leads. We also estimated with simulations and with preliminary measurements the total improvement in SNR achieved by both the more specific lead field and spatial averaging. Results obtained with simulations and with experimental measurements show an apparent improvement in SNR obtained with multielectrode leads. This encourages for future development of the method.

1. Introduction

The electroencephalogram (EEG) is traditionally measured with either unipolar or bipolar leads from the surface of the scalp. These measurements are much more sensitive to cortical than to deep EEG sources (Malmivuo and Suihko, 2004). Modern EEG equipment, comprising up to 256 channels, enable the synthesis of new kinds of measurement leads. The purpose of this study is to develop new multielectrode EEG leads being more sensitive in detecting signals generated deep in the brain. This is important especially in evoked potential studies, where the generators of potentials measured are so located. Such generators include for example brainstem auditory evoked potentials (BAEP) (Chiappa and Hill, 1997). The traditional bipolar measurement set-up is relatively insensitive to such brainstem sources and thousands of epochs must thus be averaged to obtain a reasonable signal-to-noise ratio (SNR). Great interest therefore attaches to the development of new measurement leads and methods which would promote better detection of signals generated deep in the brain.

Most of the methods previously applied to improve the SNR of such measurements comprise different signal-processing techniques designed to reduce noise by means of various temporal averaging schemes. Such approaches include for example median and weighted averaging and trimmed estimators (Davila and Mobin, 1992; Ozdamar and Kalayci, 1999; Leonowicz et al., 2005; Sörnmo and Laguna, 2005). Also wavelet-based denoising methods have been applied to improve the SNR (Causevic et al., 2005). Adaptive linearly constrained variance methods, so-called beamformers, have been applied to enhance e.g. deep epileptiform activity (Ward et al., 1999), although this approach is most often applied in solving inverse problems (van Drongelen et al., 1996; Van Veen et al., 1997). The beamformer methods resemble the present multielectrode lead approach, because both methods act as spatial filters i.e. they enhance signals generated in the target region.

In this study we investigate a method which is based on optimizing the sensitivity distribution of a multielectrode lead for deep brainstem sources. The purpose is to introduce the method and to demonstrate the benefits of multielectrode leads compared to bipolar leads. Differences in sensitivity distributions are analyzed theoretically and the increase in SNR is estimated with simulations. We have also conducted a preliminary experimental measurement to validate the simulation results obtained on improved SNR (Väisänen and Malmivuo, 2007).

2. Methods

2.1. Lead field and reciprocity theorem

We applied the lead field theory to calculate the measurement sensitivity distributions of different EEG leads (McFee and John-

* Corresponding author. Tel.: +358 40 8490162; fax: +358 3 311 64013.
E-mail addresses: outi.vaisanen@tut.fi (O. Väisänen), jaakko.malmivuo@tut.fi (J. Malmivuo).

0928-4257/$ - see front matter © 2009 Elsevier Ltd. All rights reserved.
doi:10.1016/j.jphysparis.2009.07.003

ston, 1953). According to the reciprocity theorem, the lead field in the volume conductor can be calculated by feeding a unit reciprocal current I_r to the lead (Malmivuo and Plonsey, 1995). The reciprocal current gives rise to a current density field $\mathbf{J}_L$ in the volume conductor. This current density field is the lead field, which is the sensitivity distribution of the lead.

Eq. (1) describes the relationship between the measured signal V_L in the lead, the current sources $\mathbf{J}^i$ and the lead field $\mathbf{J}_L$ in the volume conductor, when a reciprocal current I_r is applied to the lead (Malmivuo and Plonsey, 1995):

$$V_L = \frac{1}{I_r}\int \frac{1}{\sigma}\mathbf{J}_L \cdot \mathbf{J}^i dv, \tag{1}$$

where σ is the conductivity at the source location in the volume conductor.

2.2. An ideal lead field

Interest focused on signals generated in the brainstem, i.e. close to the center of the volume conductor. In this case all activity generated in other areas of the volume conductor, e.g. at the cortex, is regarded as noise. Within the brain volume the bipolar EEG lead has the highest sensitivity on the cortex (Malmivuo and Suihko, 2004). Its sensitivity distribution is thus not optimal for measuring signals generated in deeper structures. According to Eq. (1) an ideal sensitivity distribution for recording signals is such that its magnitude is concentrated at the source location and its orientation is parallel to the source orientation. To completely suppress the noise generated within the brain, the magnitude of the sensitivity distribution should be zero outside the source location. This is also the criterion for the optimal spatial filter in the beamformer methods (e.g. Eq. (12) in (Van Veen et al., 1997)). From the reciprocity theorem it is easy to understand, that this criterion can be closely achieved for superficial sources, because the sensitivity of closely separated electrodes is concentrated on the surface of the cortex. For the deep sources this criterion cannot be achieved.

When the measurement electrodes are located on the surface of the scalp, at least within the spherical head models, it is impossible to obtain a sensitivity distribution where the magnitude is concentrated at the center of the brain. Instead we assume that the best sensitivity distribution realized for deep sources is the uniform sensitivity distribution within the brain volume. By uniform sensitivity distribution we mean that its magnitude and orientation are uniform throughout the source volume.

The method for synthesizing a uniform lead field in a finite homogeneous volume conductor was introduced by Brody (1957), also described in Malmivuo and Plonsey (1995). The generation of such a lead field in the direction of the z-axis is illustrated in Fig. 1 (Malmivuo and Plonsey, 1995). In Fig. 1b an arbitrarily shaped finite homogeneous volume conductor is illustrated. In Fig. 1a it is extended in the direction of the z-axis to the cylinder which has the cross-section of the original volume conductor. The end planes of the cylinder are plated with a well-conducting material. As illustrated in Fig. 1a the extensions of the volume conductor are sliced to form isolated filaments. The slicing is done along the current flow lines, so that they are not intersected. If the resistors in Fig. 1b have the resistance equal to the corresponding volume conduction filaments outside the volume conductor in Fig. 1a, and the reciprocal current is applied through this resistor network, the lead field in the original volume conductor will be close to uniform.

We call such a lead as illustrated in Fig. 1b as a multielectrode lead because both of its terminals are composed of several electrodes. In both terminals the electrodes are connected together through the resistor network. The more electrodes are placed on the surface of the volume conductor, the more uniform the lead field is (Malmivuo and Plonsey, 1995).

The synthesization of a uniform lead field within a homogeneous spherical model is next described. First we consider a cylindrical homogeneous volume conductor with circular cross-section. To synthesize a uniform lead field the injected reciprocal current at every electrode must be incrementally proportional to $\cos\theta$, as illustrated in Fig. 2a (Malmivuo and Plonsey, 1995). θ is the angular displacement of the electrode from the negative z-axis. The uniform lead field, which is indicated with grey arrows, will be oriented in the positive z-direction. The variable resistors indicate that the reciprocal current fed to electrodes is adjusted based on the angle θ. As illustrated in Fig. 2b it may be assumed that the spherical model consists of thin cylindrical disks, which have a circular cross-section. Within each of the disks the uniform lead field in the positive z-direction can be obtained as illustrated in Fig. 2a. Also the shape of the volume conductor along the y-axis needs to be considered and the reciprocal current applied to electrodes at every thin disk must be incrementally proportional to $\cos\varphi$, where φ is the angular displacement of the disk from the xz-plane. Thus, to obtain a uniform lead field throughout the spherical volume conductor, the reciprocal current injected at each electrode needs to be incrementally proportional to:

$$I \propto \cos\theta\cos\varphi \tag{2}$$

In the present study we sought to synthesize a uniform lead field within the brain volume in a three-layer spherical head model. Kettunen and Malmivuo have shown (unpublished results), that if reciprocal currents calculated with Eq. (2) are injected to an inhomogeneous spherical head model, the lead field will be uniform within the innermost sphere. In the case of a three-layer spherical head model, the brain volume is the innermost sphere.

A significant benefit of a dense EEG array is that the multielectrode lead can be so oriented that the sensitivity distribution is parallel to the source orientation. The parallel orientation maximizes the signal amplitude according to Eq. (1).

2.3. Synthesis of a multielectrode lead

With modern digital signal processing there is no need to physically construct the resistor networks as illustrated in Figs. 1b and 2a to synthesize a multielectrode lead. Instead, the EEG can be measured as unipolar measurements with a dense EEG electrode array. The recorded signal of the multielectrode lead can be calculated either online during the measurement or offline thereafter, by adjusting the weight of each unipolar lead.

The weights of different unipolar leads are obtained based on optimization of the sensitivity distribution with Eq. (2). The noise-contaminated signal x of the multielectrode lead can be calculated with:

$$x(t) = \sum_{i=1}^{L} w_i[s_i(t) + n_i(t)], \tag{3}$$

where w_i is the weight of unipolar lead i, s_i is the signal measured with unipolar lead i, n_i is the noise in unipolar lead i and L the number of unipolar leads from which the multielectrode lead is synthesized.

When the multielectrode lead is synthesized from unipolar leads, the reference electrode used in the unipolar measurements will be included in either one of the terminals. Whether it is included in the positive or negative terminal depends on its location.

The sensitivity distribution and thus the weights of a multielectrode lead can be optimized before the EEG measurement, if the electrode locations are known. This can be accomplished for example by using an electrode cap. Thus the sensitivity distribution

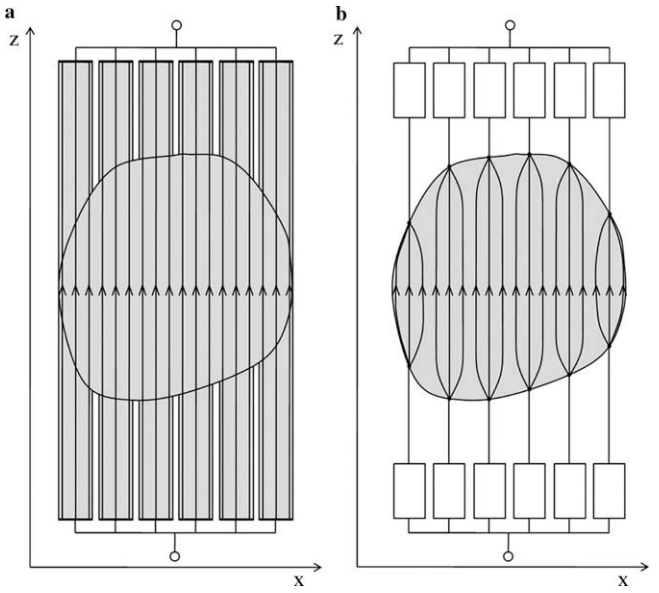

Fig. 1. Generation of a uniform lead field in a finite homogeneous volume conductor in the direction of the *z*-axis. In (a) a finite homogeneous volume conductor is extended in the direction of the *z*-axis to the cylinder which has a cross-section of the original volume conductor in (b). The extensions of the volume conductor are sliced to form isolated filaments. The slicing is so done that the reciprocal current flow lines are not intersected, as illustrated in (a). If the resistors in (b) have a resistive value equal to the volume conduction filaments outside the volume conductor in (a), and the reciprocal current is applied through this resistor network, the lead field in the original volume conductor will be close to uniform. Figure modified from Malmivuo and Plonsey (1995).

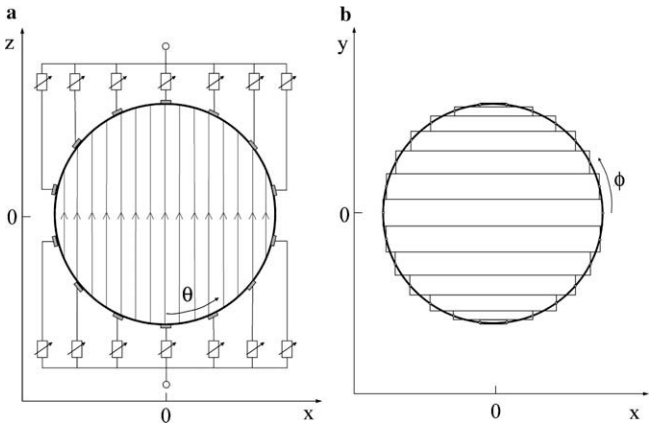

Fig. 2. Generation of a uniform lead field in a spherical volume conductor in the direction of *z*-axis. The spherical volume conductor can be approximated so as to be composed of thin cylindrical disks. In (a) a plot from the *xz*-plane is illustrated. Variable resistors reflect that the current applied to different leads is adjusted based on the angle θ. The grey arrows outline the lead field. In (b) a plot from the *xy*-plane is illustrated. φ is the angular displacement of the disk from the *xz*-plane.

optimization does not prolong the time the patient is being prepared for the measurement or the EEG data is acquired. In some EEG acquisition programs there is a possibility to form new derived channels as linear combinations of unipolar measurement channels. The multielectrode lead can be synthesized in this manner as an additional channel and its signal can be recorded simultaneously with the unipolar channels. If the quality of a multielectrode lead signal acquired online is not sufficient, the multielectrode lead can be adjusted after the EEG measurement when the original unipolar EEG data and the exact electrode coordinates have also been acquired.

2.4. Sensitivity distribution analysis

As a volume conductor model we applied the three-layer spherical head model with radii of 92 mm, 85 mm and 80 mm, respectively, as in Rush and Driscoll (1969) head model. As in (Oostendorp et al., 2000) the resistivity ratio between the tissues was 1:15:1. We applied the lead field and reciprocity theorems to calculate the sensitivity distributions within the brain volume. In the calculations we used the analytical equations derived by Rush and Driscoll (1969).

The sensitivity distributions of different leads were compared with two new parameters, the region of interest sensitivity ratio (ROISR) and the coefficient of variation of the sensitivity outside the region of interest (nonROIScv), the former of which is introduced in Väisänen et al. (2008). The nonROI volume is the source volume outside the region of interest (ROI) i.e. the brain volume outside the ROI. The ROISR defines how much more sensitive on average the detector is to individual sources in the ROI than to individual sources outside it.

$$\mathrm{ROISR} = \frac{S_k}{S_m}, \tag{4}$$

where

$$S_k = \frac{1}{K}\sum_{k=1}^{K} \|\mathbf{J}_{L_k}\|, \tag{5}$$

$$S_m = \frac{1}{M}\sum_{m=1}^{M} \|\mathbf{J}_{L_m}\|. \tag{6}$$

In (4)–(6) S_k is the average sensitivity within the ROI, k is the index of the lead vector location within the ROI, K is the total number of lead vectors calculated within ROI, S_m is the average sensitivity within nonROI, m is the index of the lead vector within nonROI and M is the total number of lead vectors calculated within nonROI. $\|\cdot\|$ is the L2-norm. According to Eq. (1), Eq. (4) is most suitable in cases where the sensitivity distribution is parallel to the source orientation. The ROISR defines how well the measurement sensitivity is concentrated within the ROI. When the sensitivity distribution is uniform, the value of the ROISR equals one.

The nonROIScv parameter defines the degree of uniformity in the magnitude of the sensitivity within the source volume outside the ROI. It is defined as the ratio between the standard deviation of the sensitivity within nonROI and the average sensitivity in the same volume.

$$\mathrm{nonROIScv} = \frac{\sigma_{S_m}}{S_m} \times 100\%, \tag{7}$$

where

$$\sigma_{S_m} = \sqrt{\frac{1}{M-1}\sum_{m=1}^{M}(\|\mathbf{J}_{L_m}\| - S_m)^2}. \tag{8}$$

In (7) S_m is the average sensitivity within nonROI, and it is calculated with Eq. (6), σ_{Sm} is the standard deviation of the sensitivity within nonROI and it is calculated with Eq. (8). When the sensitivity distribution is uniform, the value of nonROIScv equals 0%.

2.5. Theoretical multielectrode leads

We studied altogether four different theoretical leads: one bipolar and three multielectrode leads. In theoretical multielectrode lead analysis we assumed that the source is located parallel to the *z*-axis at the center of the brain. In the bipolar lead the angle

between electrodes was 180° and the electrodes were placed on the z-axis (see Fig. 2 for the coordinate system). This lead is referred to as BL from here on. The three different multielectrode leads consisted of 58, 102 and 202 electrodes. From here on these leads are called ML58, ML102 and ML202, respectively. These multielectrode leads are called as theoretical, because the point electrodes were placed as uniformly as possible over the whole spherical scalp surface. In all three multielectrode leads we first calculated the lead fields of all 57, 101 and 201 unipolar leads. All unipolar leads had the same reference electrode location (0 cm, 0 cm, −9.2 cm). The weights w_i of individual unipolar leads were calculated with Eq. (2) based on the measurement electrode location, so that the lead field of the synthesized multielectrode lead was oriented along the positive z-axis.

2.6. Preliminary experimental measurements and experimental multielectrode leads

In addition to the analysis conducted with theoretical leads we analyzed such multielectrode leads, where the electrodes are realistically distributed on the scalp surface. From here on these leads are called as experimental multielectrode leads. The realistic electrode locations were obtained from preliminary experimental measurements. These measurements were conducted to validate the SNR improvement obtained with the multielectrode lead technique. We chose to measure BAEPs (Nuwer et al., 1994), which are generated in the auditory pathway passing through the cochlear nerve, pons and midbrain. The preliminary BAEP measurements were conducted in Väisänen and Malmivuo (2007).

BAEPs were obtained from four volunteers (3 male, 1 female, mean age 28) with normal BAEP. As a stimulus we used a rarefaction click with a presentation frequency of 9.9 Hz. We stimulated the right and left ear of each testee in separate measurements, by delivering the click stimuli through a tubal phone to the ipsilateral ear, while a mask noise was presented to the contralateral ear. From each testee we collected 4000 epochs both per right ear stimulation and per left ear stimulation, resulting in two different datasets per testee. EEG was measured with a 124-channel EEG cap (SynAmps, NeuroScan, Compumedics). The measurement set-up included also the traditional BAEP electrodes placed at vertex (Cz), right mastoid and left mastoid. Depending on the stimulated ear, the mastoids are called as ipsilateral mastoid (Ai) or contralateral mastoid (Ac). The reference electrode was located on the forehead. The high-pass filter was set at 0.05 Hz and the low-pass at 2000 Hz. Subsequently and prior to the offline analysis the data were filtered with a 100 Hz high-pass filter. The time interval selected for the SNR analysis included BAEP peaks IV and V.

The electrode coordinates for each testee were digitized with Polhemus FASTRAK. Before the calculation of the lead fields and the weights w_i, the electrode positions were recentered, so that the locations best fitted the surface of the spherical head model (Delorme and Makeig, 2004). The electrodes having notably high contact impedance or signal looking extremely noisy were excluded from the multielectrode lead. The total number of electrodes in experimental multielectrode leads varied between 110 and 118, average being 114. Also artifact contaminated epochs were excluded from the analysis. The weights w_i were calculated with Eq. (2) from the recentered electrode coordinates. In the synthesized experimental multielectrode leads the number of electrodes in the negative terminal exceeded the number of electrodes in the positive terminal, because the electrodes covered the upper part of the scalp more comprehensively than the lower part.

The lead field orientation of the multielectrode lead was optimized by rotating the coordinate system. In the optimal lead, the sensitivity distribution is oriented parallel to the source orientation. Thus the lead field orientation giving the highest SNR was considered optimal. The optimization was done separately for each testee and for both simulated ear, resulting in the total of eight optimized experimental multielectrode leads.

The signal of the multielectrode lead was calculated offline after the recording with Eq. (3). All the calculations were done in Matlab. EEGLAB was applied to read the Neuroscan files into the Matlab (Delorme and Makeig, 2004). To evaluate the improvement in SNR, we compared the SNR obtained with optimized experimental multielectrode lead to the SNR obtained with bipolar BAEP lead Cz–Ai (Väisänen and Malmivuo, 2007). From the measured data the SNRs scaled for single epochs were calculated with equations adopted from Raz et al. (1988). Equations in Raz et al. (1988) estimate the power SNR, and we took the square root of the values to calculate amplitude SNRs. SNR was defined as the standard deviation of actual signal divided by the standard deviation of the noise signal.

2.7. Simulation study on spatial averaging in multielectrode leads

In the synthesis of the multielectrode lead, in addition to the uniform sensitivity distribution being more sensitive to deep sources, we also assume that spatial averaging of noise further improves the SNR. We conducted a simulation study to evaluate the effect of spatial averaging.

We simulated the brainstem evoked potentials by placing a dipolar source at the center of the brain at location (0 cm, 0 cm, 0 cm). The magnitude of the source dipole varied sinusoidally. The noise-contaminated signal of the multielectrode lead was calculated with Eq. (3) as follows. The actual signal s_i measured with each unipolar lead was calculated with Eq. (1). The measurement sensitivity of each unipolar lead to the source was thus taken into account.

After the actual signals s_i were calculated, we added Gaussian white noise (GWN) to each unipolar lead to simulate the noise n_i. Spatially uncorrelated GWN was used to model all of the different noise components. The various noise components include e.g. the background activity generated within the brain, especially on the cortex, other bioelectric signals such as electromyography (EMG), the noise generated at the skin-electrode contact and the noise coupled from the environment. In reality these components differ in amplitude and spatial properties and GWN is most suitable for modeling the non-biological noise components.

The standard deviation (SD) of n_i was kept equal in every unipolar lead. The SD of n_i was 10 times that of the actual signal measured from the lead BL. After the noisy signals ($s_i + n_i$) were generated, the noise-contaminated signal x of the multielectrode lead was calculated with Eq. (3). The SNR of simulated signals was calculated by dividing the standard deviation of the actual signal by the standard deviation of the noise signal.

2.7.1. Theoretical multielectrode leads

In the case of the leads BL, ML58, ML102 and ML202 the source dipole orientation was fixed along the positive z-axis. For each of the leads we generated 2000 noise-contaminated epochs.

2.7.2. Experimental multielectrode leads

To study the difference between the real measurements and simulations, we conducted the simulation study also with the experimental leads. Simulations were conducted both with the experimental multielectrode leads and with the traditional BAEP leads Cz–Ai. In each of the simulations, the orientation of the source dipole was set to be parallel to the optimized lead field of the experimental multielectrode lead.

3. Results

3.1. Sensitivity distribution analysis

In the sensitivity distribution analysis the lead vectors were reciprocally calculated at 2 mm intervals within the brain volume at a total of 267,730 points. As a ROI we defined a sphere of radius 1.0 cm at the center of the model. The sensitivity distributions of the theoretical leads BL, ML58, ML102 and ML202 are illustrated in Fig. 3 and the sensitivity ratios are given in Table 1. The last column gives the values for the optimal uniform sensitivity distribution.

The sensitivity distribution analysis was also conducted with the experimental leads. An example of the lead field in an experimental multielectrode lead is illustrated in Fig. 4, where the positive *x*-axis goes through right mastoid, positive *y*-axis through nasion and positive *z*-axis through vertex. The ROISR of the eight optimized experimental multielectrode leads varied between 0.936 and 0.962, average being 0.953. The nonROIScv of multielectrode leads was on average 30.1% (26.0–34.8%).

In the bipolar leads Cz–Ai, the ROISR of the eight studied leads was on average 0.829 (0.704–0.904). The nonROIScv of the bipolar lead Cz–Ai was on average 56.8% (54.0–61.0%).

3.2. SNR improvement in theoretical multielectrode leads

The characteristics of the SNR improvement obtained with multielectrode leads were studied with the theoretical leads BL, ML58, ML102 and ML202. The results of the simulation study conducted with these leads are plotted in Fig. 5, where the amplitude SNR is plotted as a function of the number of averaged epochs. It can be observed that the improvement obtained with multielectrode leads can be utilized in two different ways. The first alternative improves the quality of the signal and the second shortens the measurement time.

The point (a) corresponds to the SNR of the bipolar lead, when 2000 epochs are included in the average. If the same number of epochs is included in the average, the SNR of multielectrode leads is notably higher than that of bipolar lead. Comparing the leads ML58, ML102 and ML202 (point (b)) to lead BL, the SNR is 2.3 times, 2.9 times and 4.2 times higher, respectively. On the other hand, if the purpose is to obtain the same SNR with a multielectrode lead as with a bipolar lead, the number of epochs included in the average can be substantially reduced. The number of epochs needed with multielectrode leads to obtain a SNR similar to that by averaging 2000 epochs with lead BL, is approximately 370, 230 and 120 with leads ML58, ML102 and ML202 (point (c)), respectively.

The SNR improvement obtained through temporal averaging is approximately proportional to the square-root of the number of averaged epochs. This was expected because the noise was modeled with GWN.

The results of the simulation study show that the SNR of one epoch can be improved by increasing the number of the electrodes in the multielectrode lead. Because each unipolar lead from which the multielectrode lead is synthesized from has different measurement sensitivity to the source, the SNR improvement obtained by increasing the number of electrodes is different from the improvement obtained through temporal averaging. In the case of leads ML58, ML102 and ML202, the effect of spatial averaging is smaller than the effect of temporal averaging.

3.3. SNR improvement in experimental multielectrode leads

Examples of BAEP waveforms measured with bipolar leads and with an experimental multielectrode lead are illustrated in Fig. 6. In (a) and (b) the waveforms measured with bipolar leads from one of the testees are presented, when the right ear was stimulated. The waveform of the same signal measured with an optimal multielectrode lead is illustrated in (c). The experimental multielectrode lead is the same as in Fig. 4. In all of the Fig. 6a–c 3970 epochs, which is the maximum number of epochs included in the analysis of this dataset, are averaged to obtain the waveforms and thus the SNR is good in every lead. As observed from Fig. 6, the signal amplitude of BAEP waveform is smaller in the multielectrode lead (in (c)) than in bipolar leads ((a) and (b)), because the magnitude of the sensitivity at the center of the head is lower in a multielectrode lead than in a bipolar lead. The difference in the magnitude of sensitivity can be seen also from Fig. 3, where the sensitivity distributions of theoretical leads are illustrated.

The SNRs scaled for single epochs were analyzed for six of the measured datasets (Väisänen and Malmivuo, 2007). Two of the eight datasets discussed previously were discarded from the analysis, because of the poor contact impedance of electrode Ai. Both the SNR of the multielectrode leads and bipolar BAEP leads Cz–Ai were calculated. The SNR of six of the optimized experimental multielectrode leads was on average 0.19 (0.15–0.24) and the SNR of six of the bipolar leads Cz–Ai was on average 0.11 (0.088–0.16). Thus in the analysis of the measured data the SNR achieved with optimized multielectrode lead was on average 1.7 (1.5–2.1) times better than that of bipolar lead Cz–Ai.

The simulation study was conducted with the same six experimental multielectrode leads and bipolar leads. Because the equations adopted from Raz et al. (1988) estimate the SNR of single epochs, also in the case of simulated signals, we calculated the SNRs of single epochs. The SNR of the six of the optimized experimental multielectrode leads was on average 0.19 (0.17–0.21) and the SNR of six of the bipolar leads Cz–Ai was on average 0.084 (0.070–0.092). Thus in the simulation study the SNR achieved with optimized multielectrode lead was on average 2.3 (2.1–2.6) times better than that of bipolar lead Cz–Ai.

4. Discussion

Dense EEG electrode arrays can be applied to improve the SNR of traditional bipolar measurements. It is possible to find new bipolar leads which have a higher SNR than the traditionally applied leads. We have now in particular introduced a new multielectrode lead method which further increases the SNR of measurements made to record signals generated deep in the brain.

4.1. Effect of multielectrode leads on sensitivity distribution

We analyzed the sensitivity distributions of different leads with the ROISR and nonROIScv parameters. In multielectrode leads both the number and the distribution of electrodes affects to the values of ROISR and nonROIScv.

The value of ROISR describes the relative sensitivity of the lead to sources within the ROI. In the theoretical multielectrode leads, where the electrodes are uniformly distributed over the scalp surface, the optimal ROISR of 1.00 is achieved already with 58 electrodes (ML58). In the eight of the optimized experimental multielectrode leads the ROISR was on average 0.953, even though the average number of electrodes was 114. The ROISR is decreased because of the distribution of the electrodes. In experimental measurements an EEG cap was applied, where the electrodes cover only slightly more than half of the head surface.

The differences in sensitivity distributions were further observed by looking at the nonROIScv values. The smaller the nonROIcv, the less variation there is in the magnitude of sensitivity outside the region of interest i.e. the more uniform the sensitivity

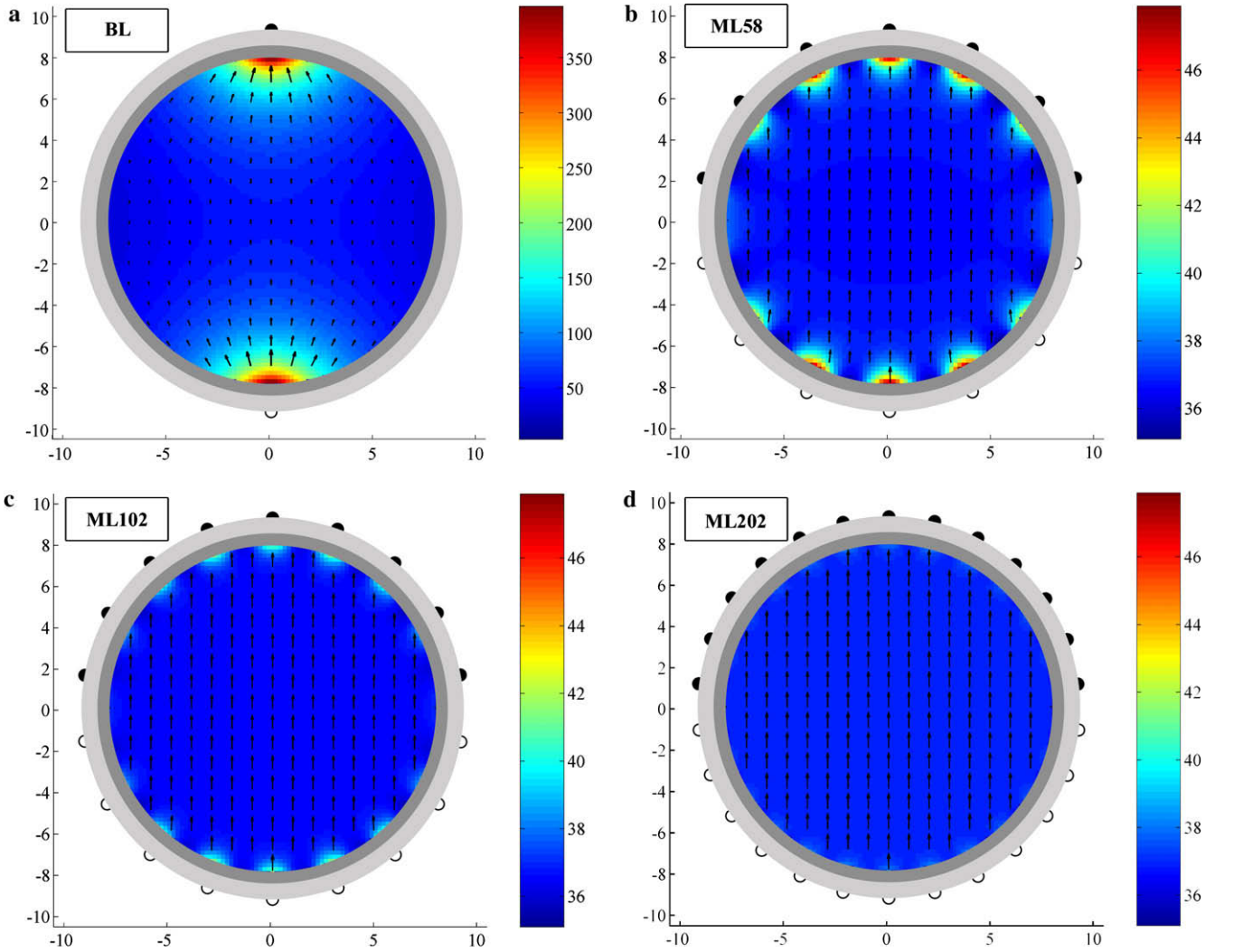

Fig. 3. Sensitivity distribution illustrated with lead vectors within the brain plotted on the *xz*-plane in leads (a) BL, (b) ML58, (c) ML102 and (d) ML202. Colorscale gives the magnitude of the sensitivity distribution $\mathbf{J}_L$ (A/m^2). The positive reciprocal current is applied to white electrodes and the negative to black electrodes. In (b–d) weights for unipolar leads are calculated according to Eq. (2). Note that the scaling in the sensitivity distributions is different in (a) than in (b–d).

Table 1
Calculated sensitivity ratios for theoretical EEG leads. In the fifth column the values for a uniform lead field are given. The ROI is defined as a sphere with a radius of 1 cm at the center of the brain.

Lead	BL	ML58	ML102	ML202	Ideal ML
Electrodes	2	58	102	202	∞
ROISR	0.953	1.00	1.00	1.00	1.00
nonROIScv (%)	48.8	2.18	0.93	0.30	0.00

distribution is. The nonROIScv values of theoretical multielectrode leads with uniformly distributed electrodes were below 3%. In experimental multielectrode leads on the other hand the nonROIScv was on average 30.1%. From the ROISR and nonROIScv values we can conclude that to obtain optimal sensitivity distribution with high ROISR and low nonROIScv value, the number of electrodes in a multielectrode lead needs to be high and the electrodes should be distributed as uniformly as possible.

4.2. Effect of lead field optimization

In the experimental multielectrode leads the realistic electrode locations were fitted on the surface of a three-layer spherical head model, and the measurement sensitivity distribution was optimized based on Eq. (2). Also the weights were calculated as if the electrodes were uniformly distributed over a spherical surface. This optimization method does not necessarily result in the most optimal sensitivity distribution for deep sources. By visual evaluation of Fig. 4 and by investigation of the nonROIScv values, it can be observed that sensitivity distributions of the experimental multielectrode leads are less optimal than those of theoretical multielectrode leads (Fig. 3b–d) but still improved compared to bipolar leads (Fig. 3a).

When the lead field of a multielectrode lead is optimized for deep sources, the goal is to synthesize a uniform sensitivity distribution. If the sensitivity distribution is uniform, the lead is equally sensitive to sources located at different depths if the source orientation is kept fixed. Thus a deviation of the deep source location from the center of the model does not affect to the SNR obtained with the lead. As illustrated in Fig. 3, the sensitivity distribution of theoretical multielectrode leads is uniform almost throughout the whole brain volume. From Fig. 4 it can be seen that the sensitivity distribution of experimental multielectrode leads is less uniform than that of theoretical leads. Thus the SNR of the lead is changed, if the source is not located right at the center of the model.

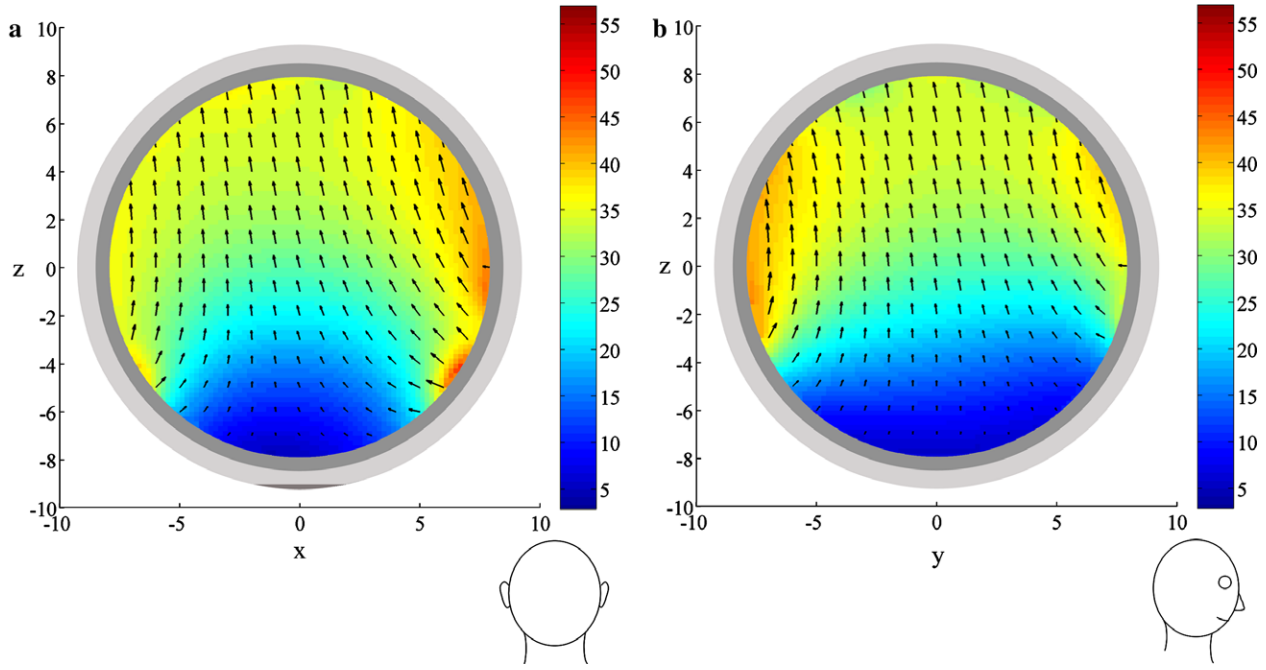

Fig. 4. Sensitivity distribution of an experimental multielectrode lead illustrated with lead vectors within the brain plotted on the (a) *xz*-plane and (b) *yz*-plane. Colourscale gives the magnitude of sensitivity distribution $\mathbf{J}_L$ (A/m^2).

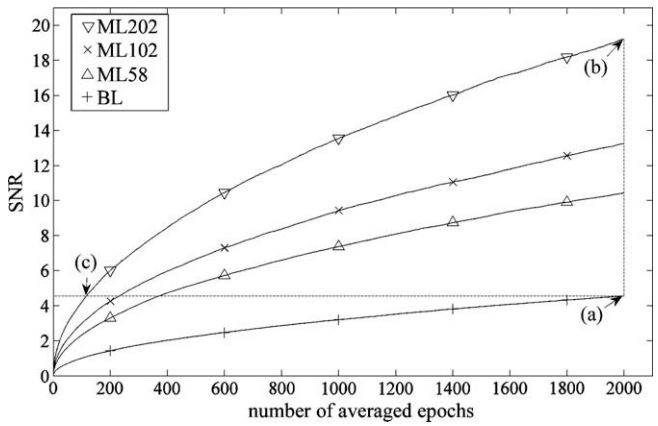

Fig. 5. SNR of different theoretical EEG leads plotted as a function of the number of averaged epochs. The point marked with (a) corresponds to the SNR of the traditional bipolar EEG, when 2000 epochs are included in the average. The improvement obtained with multielectrode leads can be utilized in two different ways, illustrated with grey dashed lines. If the same number of epochs is included in the average, the SNR of multielectrode leads is notably higher than that of bipolar lead (a → b). If the purpose is to obtain the same SNR with a multielectrode lead as with a bipolar lead, the number of epochs included in the average can be substantially reduced (a → c).

We evaluated the effect of deep source location on SNR by moving the source dipole within a 2 cm radius from the center of the model in the experimental multielectrode leads. When the source was moved within the 2 cm radius, the SNR was on average the same as when the source was located at the center of the model. When the source location was moved the SNR was at minimum 78% and at maximum 117% of the average SNR. It also has a slight effect on the SNR, whether the source was moved orthogonal or parallel to the lead field orientation. In the former case the variation in SNR is smaller than in the latter case. When the source was moved orthogonal to the lead field orientation, the SNR was on average 101% of the SNR, when the source was located at the center of the model. When the source was moved parallel to the lead field orientation, the SNR was on average 98% of the SNR, when the source was located at the center of the model. The decrease in SNR, when the source is moved parallel to the lead field orientation is caused by the decrease in the magnitude of the sensitivity distribution towards the neck, as illustrated in Fig. 4.

A great concern, when considering the deep sources and the synthesization of an optimal sensitivity distribution, is the effect of the head model applied. In the present study we applied the spherical head model because we wanted to evaluate the phenomena behind the improved SNR. Within the spherical head model the optimal uniform sensitivity distribution can be synthesized when the weights for the electrodes are calculated with Eq. (2). The realistically shaped head models are always specific for certain head geometry. Thus the weights needed for the synthesization of an optimal sensitivity distribution, as well as the optimal sensitivity distribution itself, will be different for each individual head geometry. The biggest drawback of the spherical head models is that the deep structures of the brain are not correctly modeled. These include, for example, the ventricles around the brainstem, which have a particularly clear effect on the lead field patterns. Thus for the accurate calculation of the sensitivity distribution the head should be modeled with individual realistically shaped model in the future studies. In this case also a new optimization method needs to be developed to define the weights for the unipolar leads from which the multielectrode lead is synthesized.

4.3. Improvement of SNR with multielectrode leads

In the experimental multielectrode leads the number of electrodes was on average 114. In the simulation study the SNR of these multielectrode leads was lower than the SNR achieved with theoretical multielectrode lead ML58, which consists of notably lower number of electrodes uniformly distributed on the spherical scalp surface. This in addition to the evaluation of ROISR and nonROIScv values emphasizes the need for the development of new electrode montages and sensitivity distribution optimization methods.

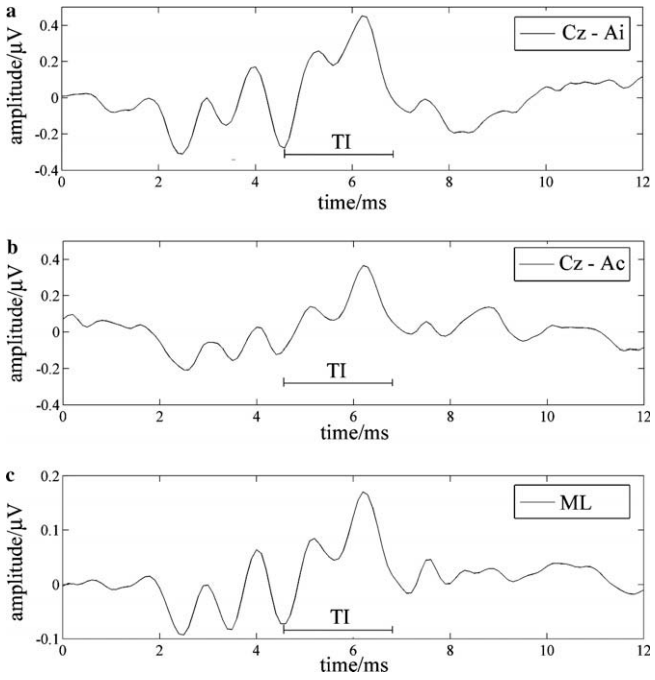

Fig. 6. Example BAEP waveforms. The stimulus was delivered to right ear and 3970 epochs are averaged. (a and b) original BAEP waveforms, (c) BAEP waveform of optimized multielectrode lead (ML). The sensitivity distribution of the multielectrode lead is illustrated in Fig. 4.The studied time interval (TI) includes the peaks IV–V.

In the experimental measurements the SNR achieved with optimized multielectrode leads was on average 1.7 times better than that of bipolar lead Cz–Ai (Väisänen and Malmivuo, 2007). The amplitude SNR improvement by a factor of 1.7 means, that instead of averaging 2000 epochs with a bipolar lead, it is sufficient to average 690 epochs with a multielectrode lead to obtain similar SNR. When the simulation study was conducted with the same experimental leads, the SNR of multielectrode lead was on average 2.3 times better than that of bipolar lead Cz–Ai. Thus the SNR improvement achieved in experimental measurements was 75% of the improvement achieved in the simulation study.

The main reason for the better SNR improvement obtained in simulations than in experimental measurements was caused by applying an oversimplified noise model in the simulation study. In future investigations the different components of noise should be studied separately, because these components differ in amplitude and spatial properties. As the electrodes are located closer to each other, especially the noise signals generated on the cortex will be correlated over many electrodes (Nunez et al., 1997; Srinivasan et al., 2007). At low frequencies the correlation over different electrodes distances is higher than at high frequencies (Srinivasan et al., 2007). The correlation is caused by both the genuine correlation of cortical sources and the correlation that arises due to volume conduction. At low frequencies the correlation arises due to both of these factors, but at higher frequencies (>30 Hz) the correlation arises mainly due to volume conduction, since the cortical sources at these frequencies are apparently uncorrelated (Srinivasan et al., 2007). In the frequency band which is used to measure BAEPs (>100 Hz), the background EEG might thus be mainly uncorrelated. However, because of the shown volume conductor effects, in the future studies the noise measured from the scalp surface, which is generated within the brain, should be modeled with spatially correlated noise. The correlation of other noise components should also be investigated. When the correlation increases, the efficiency of spatial averaging on improving the SNR will decrease. However, if the number of electrodes is increased by covering the head more comprehensively, the electrode density remains constant. The efficiency of spatial averaging is a complicated process which strongly depends on the relative magnitudes of the correlated and non-correlated noise sources, which may differ notably between different measurements.

4.4. Multielectrode lead method and beamformers

The present multielectrode lead method can be considered as a spatial filtering method. Other widely studied spatial filtering methods include the beamformer methods which provide another means to optimize measurements for sources at different depths within the brain (van Drongelen et al., 1996; Van Veen et al., 1997; Ward et al., 1999). The multielectrode lead Eq. (3) is the same as the output equation of the beamformers (Van Veen et al., 1997). The difference between these two methods is in the selection of the weights w_i. Because for deep EEG sources it is impossible to have such a weighted lead field where the magnitude is one at the source location and zero elsewhere, in beamformers the former of these criteria is preserved, while the effect of noise is suppressed by minimizing the variance of the beamformer output. The selection of the weights is made based on the statistics of the measured data and on the lead vector magnitudes only at the source location (Van Veen et al., 1997).

In the multielectrode lead method, the weights are defined based on the optimized lead field i.e. the lead vectors at all locations within the brain, not only at the source location. The lead field is optimized by maximizing the relative sensitivity at the source location. Present multielectrode lead method results in the optimal improvement for deep EEG sources, when the noise sources are uniformly distributed within the brain.

A great benefit of the present multielectrode lead method is its simplicity. There is no need to estimate the covariance matrix of the measured signals as in beamformers (Van Veen et al., 1997), but it is adequate to only calculate and optimize the lead fields. The multielectrode lead method is also more illustrative, since the best reachable sensitivity distribution in magnitude and direction for deep sources can be visualized. Also the weights can be defined prior to the EEG measurement is conducted.

4.5. Measurement with dense EEG arrays

The improvements obtained in the present study encourage for future developments of the method. We assume that the SNR obtained with weighted multielectrode leads can be further improved by first of all developing new electrode montages. These new electrode montages should cover the lower part of the head more comprehensively than traditional EEG montages. Secondly, the optimization of the sensitivity distribution is assumed to be further improved by applying individual realistically shaped head models and new optimization methods to synthesize the optimal sensitivity distribution within realistically shaped head models.

A drawback at the moment with dense EEG arrays is the time-consuming task of applying the electrodes. So long as this process remains as slow as today, the extra time needed to attach a large number of electrodes properly will exceed the time saved with shorter recording time with multielectrode leads. However, new technologies such as amplifiers with higher input impedances and active electrodes will notably cut down the application time.

The new multielectrode leads will bring many benefits to EEG studies. Among the first applications are evoked potential studies, where fewer epochs are sufficient for an average without reducing the signal quality. This is important if the response signal tends to change as the number of stimuli is increased. Such changes might arise due to fatigue, learning habituation or other factors. New multielectrode leads more sensitive to measure deep EEG sources

might also reveal new features of brain activity in spontaneous recordings.

5. Conclusions

In the present study we have developed a multielectrode lead technique that can be applied to improve the SNR of EEG generated by deep brainstem sources.

We showed with a theoretical approach how the sensitivity distribution of a weighted multielectrode lead should be optimized for deep EEG sources. With simulations we showed that the SNR is improved with multielectrode leads compared to traditional bipolar leads. The improvement of the SNR was validated with preliminary experimental BAEP measurements. In the experimental measurements the amplitude SNR of multielectrode lead was on average 70% higher than the SNR obtained with traditional bipolar lead. To conclude, the SNR of the EEG measurements can be improved with the present weighted multielectrode lead method compared to traditional bipolar leads, when the signals are generated deep in the brain.

Acknowledgements

This work has been supported by the Finnish Cultural Foundation, the Graduate School of Tampere University of Technology and the Academy of Finland.

References

Brody, D.A., 1957. A method for applying approximately ideal lead connections to homogeneous volume conductors of irregular shape. Am. Heart. J. 53, 174–182.

Causevic, E., Morley, R.E., Wickerhauser, M.V., Jacquin, A.E., 2005. Fast wavelet estimation of weak biosignals. IEEE Trans. Biomed. Eng. 52, 1021–1032.

Chiappa, K., Hill, R., 1997. Brainstem auditory evoked potentials: interpretation. In: Chiappa, K. (Ed.), Evoked Potentials in Clinical Medicine. Lippincott-Raven, Philadelphia, pp. 199–249.

Davila, C.E., Mobin, M.S., 1992. Weighted averaging of evoked potentials. IEEE Trans. Biomed. Eng. 39, 338–345.

Delorme, A., Makeig, S., 2004. EEGLAB: an open source toolbox for analysis of single-trial EEG dynamics including independent component analysis. J. Neurosci. Methods 134, 9–21.

Leonowicz, Z., Karvanen, J., Shishkin, S.L., 2005. Trimmed estimators for robust averaging of event-related potentials. J. Neurosci. Methods 142, 17–26.

Malmivuo, J., Plonsey, R., 1995. Bioelectromagnetism: Principles and Applications of Bioelectric and Biomagnetic Fields. Oxford University Press, New York.

Malmivuo, J.A., Suihko, V.E., 2004. Effect of skull resistivity on the spatial resolutions of EEG and MEG. IEEE Trans. Biomed. Eng. 51, 1276–1280.

McFee, R., Johnston, F.D., 1953. Electrocardiographic leads. I. Introduction. Circulation 8, 554–568.

Nunez, P.L., Srinivasan, R., Westdorp, A.F., Wijesinghe, R.S., Tucker, D.M., Silberstein, R.B., Cadusch, P.J., 1997. EEG coherency. I: statistics, reference electrode, volume conduction, Laplacians, cortical imaging, and interpretation at multiple scales. Electroencephalogr. Clin. Neurophysiol. 103, 499–515.

Nuwer, M.R., Aminoff, M., Goodin, D., Matsuoka, S., Mauguiere, F., Starr, A., Vibert, J.F., 1994. IFCN recommended standards for brain-stem auditory evoked potentials. Report of an IFCN committee. International Federation of Clinical Neurophysiology. Electroencephalogr. Clin. Neurophysiol. 91, 12–17.

Oostendorp, T.F., Delbeke, J., Stegeman, D.F., 2000. The conductivity of the human skull: results of in vivo and in vitro measurements. IEEE Trans. Biomed. Eng. 47, 1487–1492.

Ozdamar, O., Kalayci, T., 1999. Median averaging of auditory brain stem responses. Ear. Hear. 20, 253–264.

Raz, J., Turetsky, B., Fein, G., 1988. Confidence intervals for the signal-to-noise ratio when a signal embedded in noise is observed over repeated trials. IEEE Trans. Biomed. Eng. 35, 646–649.

Rush, S., Driscoll, D.A., 1969. EEG electrode sensitivity – an application of reciprocity. IEEE Trans. Biomed. Eng. 16, 15–22.

Sörnmo, L., Laguna, P., 2005. Bioelectrical Signal Processing in Cardiac and Neurological Applications. Academic press, New York.

Srinivasan, R., Winter, W.R., Ding, J., Nunez, P.L., 2007. EEG and MEG coherence: measures of functional connectivity at distinct spatial scales of neocortical dynamics. J. Neurosci. Methods 166, 41–52.

Väisänen, O., Malmivuo, J., 2007 Improved detection of deep sources with weighted multielectrode EEG leads. In: 29th Annual International Conference of the IEEE Engineering in Medicine and Biology Society, Lyon, France, pp. 5194–5197.

Väisänen, J., Väisänen, O., Malmivuo, J., Hyttinen, J., 2008. New method for analysing sensitivity distributions of electroencephalography measurements. Med. Biol. Eng. Comput. 46, 101–108.

van Drongelen, W., Yuchtman, M., Van Veen, B.D., van Huffelen, A.C., 1996. A spatial filtering technique to detect and localize multiple sources in the brain. Brain. Topogr. 9, 39–49.

Van Veen, B.D., van Drongelen, W., Yuchtman, M., Suzuki, A., 1997. Localization of brain electrical activity via linearly constrained minimum variance spatial filtering. IEEE Trans. Biomed. Eng. 44, 867–880.

Ward, D.M., Jones, R.D., Bones, P.J., Carroll, G.J., 1999. Enhancement of deep epileptiform activity in the EEG via 3-D adaptive spatial filtering. IEEE Trans. Biomed. Eng. 46, 707–716.